

DTIC FILE COPY

4

MT-CWR-088-022

ANNUAL REPORT

**Investigations into the Infiltration Kinetics and Interfacial
Bond Strength of Al/SiC Composites**

Contract N00014-88-K-0500

Submitted to:

Dr. Steven Fishman
Office of Naval Research
800 North Quincy Street
Arlington, Virginia 22217

DTIC
ELECTE
OCT 25 1988
S D
C/D

AD-A200 752

Submitted by:

Glen R. Edwards and David L. Olson
Center for Welding and Joining Research
Colorado School of Mines
Golden, Colorado 80401

ABSTRACT STATEMENT A
Approved for public release
Distribution Unlimited

July, 1988

CSM



CENTER FOR **W**ELDING **R**ESearch
Colorado School of Mines
Golden, Colorado 80401

88 1012 069

TABLE OF CONTENTS

.0 PROJECT OVERVIEW. 1

.0 POROUS COMPACTS 3

.0 SEMI-EMPIRICAL TECHNIQUE FOR MEASURING BOND STRENGTH
AND WETTABILITY AT THE METAL/CERAMIC INTERFACE. 9

.0 FUTURE WORK 27

.0 ACKNOWLEDGEMENTS. 29

.0 REFERENCES. 30

PPENDIX I 34

PPENDIX II. 44

Accession For	
NTIS CRA&I	<input checked="" type="checkbox"/>
DTIC TAB	<input type="checkbox"/>
Unannounced	<input type="checkbox"/>
Justification	
By <i>per ltr</i>	
Distribution	
Availability Codes	
Dist	Avail and/or Special
A-1	



1.0 PROJECT OVERVIEW

The work for this project is continuing in the following two areas: 1) isothermal infiltration into porous compact and tube bundles or capillaries and 2) a fundamental study of bonding at the metal ceramic interface. The porous compact study is a continuation of previous work (1) from which a paper was submitted to Met. Trans. B for publication. Another paper on the mathematics of fluid flow behavior in porous compact media has been published (2). In the last year, the emphasis in the porous compact study has been to characterize pre-infiltration incubation times as well as infiltration rates. The results of preliminary findings, along with the work on particle coatings (to enhance infiltration), will be presented.

Experiments are continuing with the tube bundle/capillary geometry, where both static rise (to determine $\gamma_{LV} \cos\theta$) and dynamic infiltration tests are being conducted. The configuration of the 200- μm -diam. capillaries in the dynamic infiltration tests is such, that once infiltrated, a measurement of interfacial shear strength can be made. Trial infiltration of molten aluminum into SiC capillaries has produced measured rates more than 50% faster than the rates predicted by model calculations (2). A new, more accurate pressure control and delivery system was installed and better agreement between measured and predicted rates in future tests is anticipated.

In a continuing effort to understand the fundamental nature of the ^{Al/SiC} Al/SiC interface, a technique for determining properties at the metal/ceramic interface was proposed. The model provides a method for predicting interfacial properties from the measured optical properties of the metal and ceramic surfaces. A review of this model is included.

Project research over the last year has involved extensive developmental work. A new apparatus for infiltrating porous compacts with molten metals has

been devised and constructed. Better pressure control and regulation have been implemented, and the original apparatus has been upgraded to include these modifications.

2.0 POROUS COMPACTS

This project has studied the isothermal infiltration of uncoated and coated-and-sintered silicon carbide porous compacts by molten aluminum. The ongoing work has examined some facets of infiltration behavior including incubation times and activation energies.

A hypothesis for explaining the incubation times shown in the 1987 annual report has been developed. It is suggested that the compact undergoes pre-conditioning before the initiation of infiltration, and the mechanism by which this occurs is shown schematically in Figure 1. As the planar liquid aluminum front contacts the face of the porous compact, the liquid interface begins to deform, and develops significant curvature as the liquid intrudes into the interstices (pores) between the silicon carbide particles. The resulting capillarity increases the vapor pressure of aluminum in the pores of the compact in accordance with the equation given below:

$$P_V - P_{V\infty} = \frac{2\gamma_{LV}}{r}; \quad r_p \leq r < \infty \quad (1)$$

where P_V = equilibrium vapor pressure above a curved surface,
 $P_{V\infty}$ = equilibrium vapor pressure above a flat surface, γ_{LV} =
 liquid-vapor surface tension, r = radius of curvature for the liquid surface,
 and r_p = radius of pores in the compact.

For a 10- μm pore radius, the vapor pressure of pure aluminum at its melting point is increased from approximately 10^{-6} Pa to approximately 100 kPa. The increased partial pressure of aluminum in the gas phase leads to an increased reaction rate between aluminum and the surface of the silicon carbide particles, which conditions the surface and promotes infiltration. This capillarity-driven process which conditions the silicon carbide particles

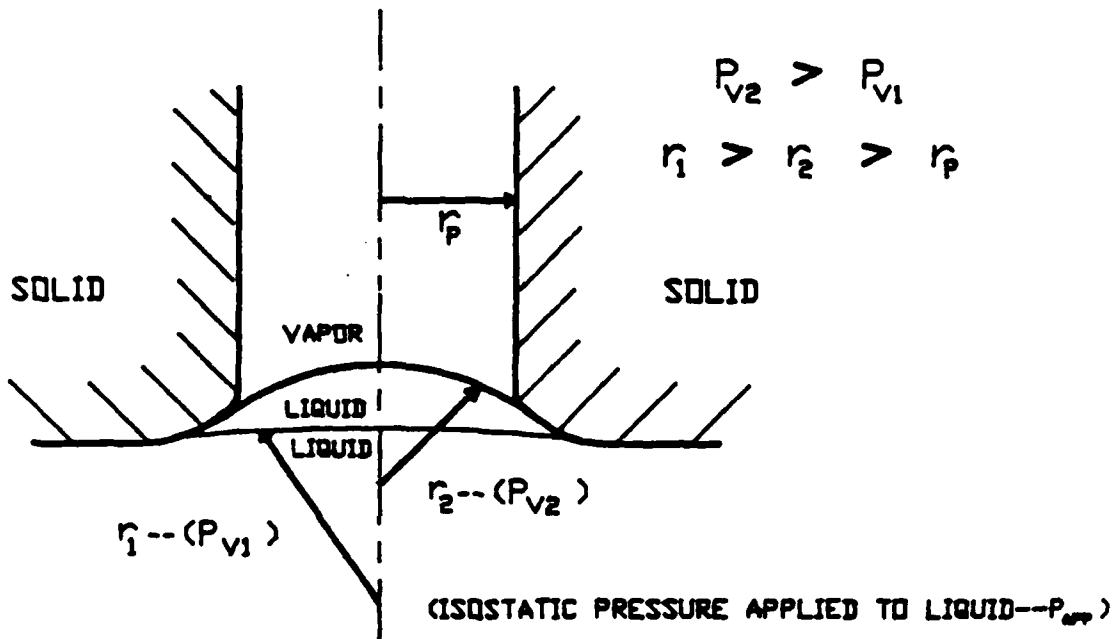


Figure 1. Schematic of mechanism explaining the pre-conditioning of a porous compact before the initiation of infiltration.

is a possible explanation for the observed incubation times discussed in the 1987 annual report.

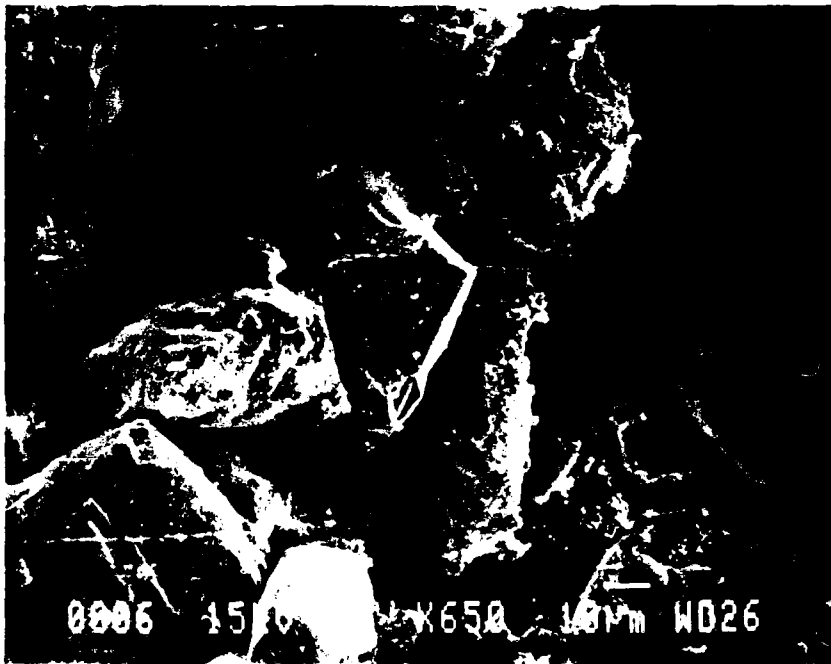
Metallic coatings are expected to enhance the wetting of the ceramic particles by aluminum, and hence, reduce incubation times. Copper coatings have successfully been electroless plated onto silicon carbide particles. Results of these coating experiments are shown in Figure 2a. The kinetics of copper dissolution into molten aluminum have been considered. The following relation can be used to describe this behavior:

$$R(t) - R_0 = \frac{-K_m^1}{\delta_{Cu}} \cdot t \quad (2)$$

where $R(t)$ = radius of the copper coated spherical particle at dissolution time T , R_0 = initial radius of the copper coated spherical particle, K_m^1 = apparent dissolution reaction rate coefficient, δ_{Cu} = density of copper, and t = dissolution time.

This model considers the dissolution process to be diffusion controlled, and it also considers the saturated concentration of the copper in aluminum at the interface to be much greater than the concentration of copper in the bulk solution (i.e. the bulk concentration is close to zero). The dissolution time at 704°C is 0.33 seconds, and at 760°C, the time is 0.20 seconds. In light of this information, it should be noted that the copper coatings on the silicon carbide particles should dissolve into the aluminum very shortly after infiltration of the compact occurs.

In addition, it has been found that particle redistribution occurs during infiltration, resulting in a difference in calculated and measured infiltration rates at applied pressures much greater than the threshold pressure. Consequently, an effort is being conducted to sinter the coated



(a)



(b)

Figure 2. (a) Electroless copper coatings on 5 μ silicon carbide particles (magnification = 650X). (b) Copper-coated silicon carbide particles that have been sintered using the copper coating as a binder (magnification = 650X).

powder compacts before infiltration. The copper coatings appear to act as a satisfactory binder as shown in Figure 2b, but the coatings also agglomerate resulting in a less uniform coating.

Further analysis of the incubation time has also been attempted, and an activation energy for the above mechanism has been determined for the preliminary data available. If the process is considered a zero order reaction (with respect to the species on the SiC surface), the activation energy can be calculated (for constant applied pressure) from the following equation:

$$1/t_0 = A [\exp (-Q/RT)] \quad (3)$$

where: t_0 = incubation time, A = pre-exponential factor, Q = activation energy, R = gas constant, and T = absolute temperature ($^{\circ}K$).

Using the data from Figure 3, an activation energy of approximately 18 kcal/gmole has been determined.

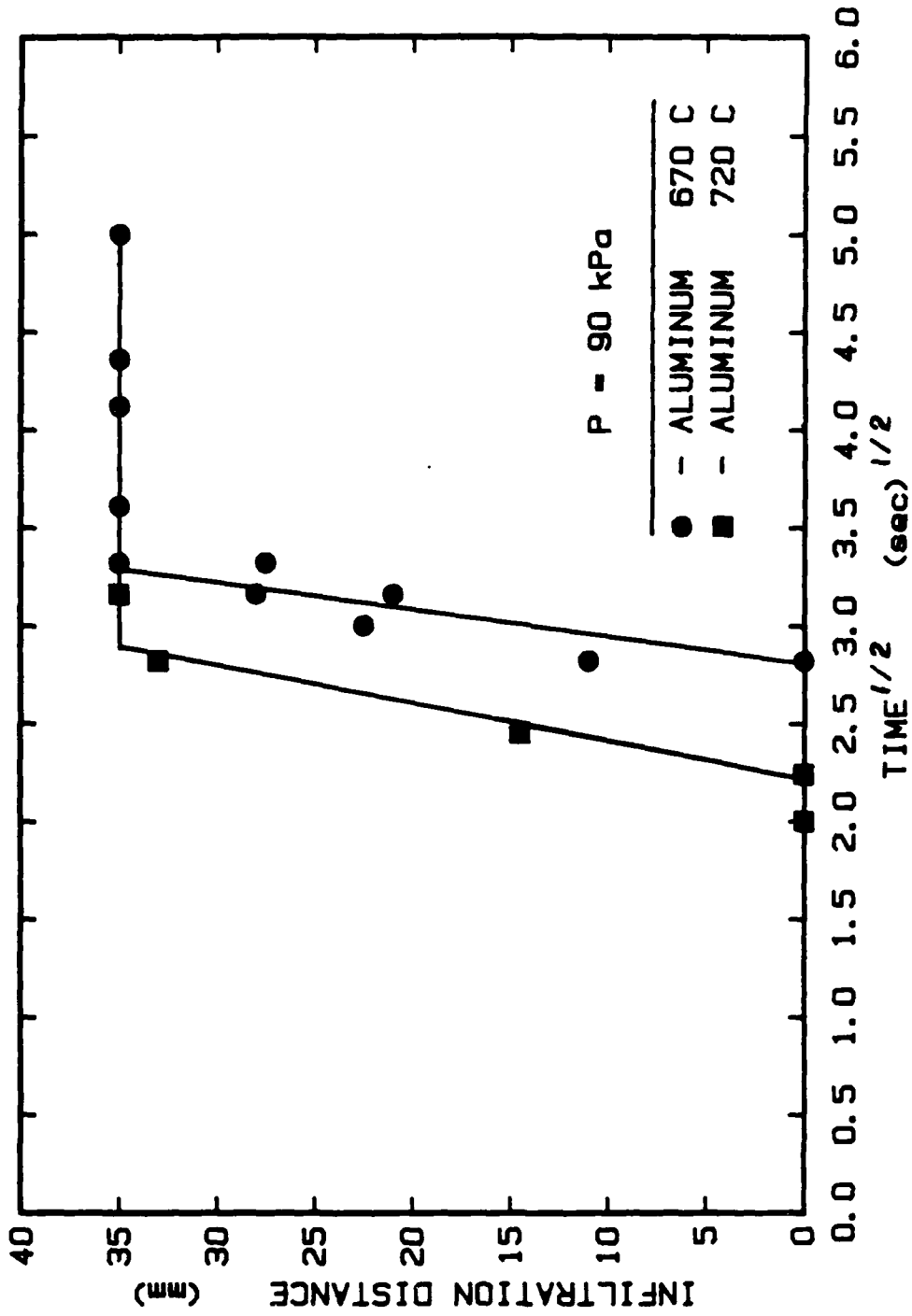


Figure 3. Typical infiltration rate measurements from the infiltration of molten aluminum into a porous compact of silicon carbide particles.

3.0 SEMI-EMPIRICAL TECHNIQUE FOR MEASURING BOND STRENGTH AND WETTABILITY AT THE METAL/CERAMIC INTERFACE

Investigations into the nature of the interfacial bond reveal the difficulty of finding a practical, unified model to adequately predict properties of any generic interface. Theoretical models, such as Ferante and Smith's universal bonding model for metal (3), are conceptually simple, but actual calculations are extensive and complex, and in some cases, the predicted variables or "observables" are not even measurable. The more practical models, with measurable parameters, are typically empirical or semi-empirical and limited to specific A-A or A-B atom combinations. To predict accurately and practically the properties of an interface, the interfacial structure must be established by a single type of bonding; whether it be covalent, ionic, metallic, or Vander Waal type bonding. In the event that more than one bonding type is present, the accuracy or predictability of any one model is suspect.

Bonding at the metal/ceramic interface, which is of primary concern in metal matrix composites, can be dominated by any one of the common bonding types. The approach then has been to find a practical unified model which can be used to predict interfacial properties in terms of measurable electronic parameters. Out of the literature cited, the pioneering work of Phillips (4,5) for Group IV semiconductor materials was considered a practical, accurate framework from which to build a predictive model; the semiconductor is unique in that it is insulating at low temperatures and conducting at high temperatures and will provide a basis for correlating electronic structural behavior to interfacial properties.

The models of a particular bonding type can provide insight into the development of an overall bonding model. Hence, a review of relevant metallic

<u>MODEL</u>	<u>VOLUME DEPENDENT ENERGY</u>	<u>ELECTROCHEMICAL POTENTIAL ENERGY</u>
i) Hume-Rothery (solid solution alloy formation)	15% size rule	"electronegative" valence effect
ii) Pauling $\Delta H_{(AB)} \propto 23M(\chi_A - \chi_B)$	# of resonating bonds M	electronegativity of atom i, χ_i
iii) Friedel (Transition metals)	SIZE FACTOR (elastic continuum model)	"d" electron bonding (charge transfer from compound with higher E_f)
iv) Miedema (analogous to energy-density functional approach of Girifalco $\Delta H_{(AB)} \propto f(c) [-P(\Delta\Phi)^2 + S(\Delta n_{W/S})^{2/3} - R]$	electron density at W/S boundary, $\Delta n_{W/S}$ [†]	work function, $\Delta\Phi$

[†] Note: According to Girifalco, $\Delta n_{W/S}$ is the change in cohesive energy when W/S cells are either expanded or compressed ('elastic' or size effect).

Figure 4. Summary of metallic bonding models.

$$\Delta H_{AB} = \Delta H_0 \left(\frac{d_{0c}}{d_{AB}} \right)^s f_{i(AB)} D$$

Where:

ΔH_0 = scaling constant

$\left(\frac{d_{0c}}{d_{AB}} \right)^s$ = covalent energy not lost by dehybridization

f_i = ionic ordering energy; "energy for ions A and B to form two interpenetrating lattices" (\propto Madelung energy)

D = dehybridization parameter; "energy lost by dehybridization of the d orbitals"

Parameters are determined in terms of the measured energy gaps at symmetry points.

Figure 5. Phillips: A semi-empirical bonding model in terms of interband energy gaps (for group IV tetrahedrally coordinated compounds).

and covalent bonding models was completed (a brief, condensed table of the models is given in Figures 4 and 5). With respect to interfacial properties, these models pertain to the solid state; i.e. solid A atoms interacting with solid A or solid B atoms. Solid-liquid interactions, which occur during the processing or fabrication of metal/ceramic composites, represent a separate challenge to predicting properties of the metal/ceramic interface. Therefore, an additional review was completed on the energetics of the solid/liquid interface with reference to the infiltration or wettability behavior (refer to the infiltration/wettability section in Appendix I).

The final aspect of the proposed model is the link between the final properties at the solid/solid interface and the initial factors which control infiltration or wettability at the solid/liquid interface. Using surface free energies and the concept of work of adhesion between two free surfaces, an expression for interfacial bond strength and wetting was developed. For each of the surface free energy terms, a correlation to an enthalpies of formation was developed by Miedema (6,7) and these correlations were used in this development (refer to the section on bonding at the metal/ceramic interface in Appendix II).

The novelty of the approach used in this study is in the determination of enthalpies of formation (and surface free energies) of compounds and interfaces with an optical reflectance technique. Static optical reflectance techniques traditionally have been used to measure characteristic valence interband transition energies in semiconductors, and Phillips used these "optically-generated" characteristic transition energies to calculate formation energies in Group IV semiconductors. The objective in the work is to use a modulation reflectance technique to enhance characteristic interband transitions in not only semiconductors but other types of compounds such as

metal alloys and metal/ceramic interfaces. Although the electronic behavior in polyvalent metals (i.e. aluminum) is nearly free and delocalized, it will be shown that characteristic electronic transitions, known as "parallel-band" effects, do occur in these metals and that these transitions can be correlated to enthalpies of formation and surface energies. Hence, for any generic metal/ceramic interface, we anticipate being able to determine the interfacial bond strength and the liquid/solid wettability from the characteristic interband transitions generated in the modulated reflectance spectra.

The accomplishments in the development of this model over the last year have therefore been:

1. Incorporation of polyvalent metal behavior into the framework of Phillips original semiconductor model.
2. Proposal of an optical technique, i.e. modulation reflectance spectroscopy, to measure electronic behavior in both semiconductors, metals, and metal/semiconductor interfaces.
3. Proposal of an optical technique to measure changes in surface and interfacial bonding behavior as a result of contamination from impurities, such as oxides.

3.1 Theoretical Considerations

Since the objective in this research is to improve the fundamental understanding of the infiltration process as well as the interfacial bond in aluminum matrix-silicon carbide composites, the theoretical aspects of the proposed model have been broken into two areas. The first area concerns

infiltration kinetics; the second area considers the interfacial bond strength. The modeling of the infiltration kinetics has already been presented in previous reports and will not be repeated here. Again, the emphasis will be to develop fundamental parameters in the metal/ceramic system which can be used to predict a priori the infiltration kinetics during processing and the ultimate bond strength of the finished product.

3.1.1 Interfacial Bond Strength (Determination of Enthalpies of Formation)

An extensive review of "practical" metal/semiconductor bonding models was completed and the more prominent models were presented in Figures 4 and 5. The models were categorized as relating to bonding in either metals or semiconductors. Since an objective of this research is to predict infiltration behavior and interfacial bond strength of metal matrix composites prior to processing, the proposed model will be developed in terms of the individual constituents (i.e. metal or ceramic) as opposed to the final products that may form at the interface. By definition, a model should "predict" or represent a phenomenon in terms of known fundamental properties. Therefore, for this research it is important to understand the emphasis on the original (fundamental) constituents as well as for the final interfacial properties.

The metal/semiconductor interfacial region is complex, with chemically-reacted and/or diffused regions, local charge redistribution, built in potential gradients, and newly created dielectric properties. Hence, it would be naive to believe that a knowledge of the electronic structure or properties of this complex interface could be extracted from just the ideal, bulk properties of the individual constituents. Initially, this model will treat the metal/semiconductor interface as an abrupt contact, but then will be extended to treat the interface as an "interphase" region.

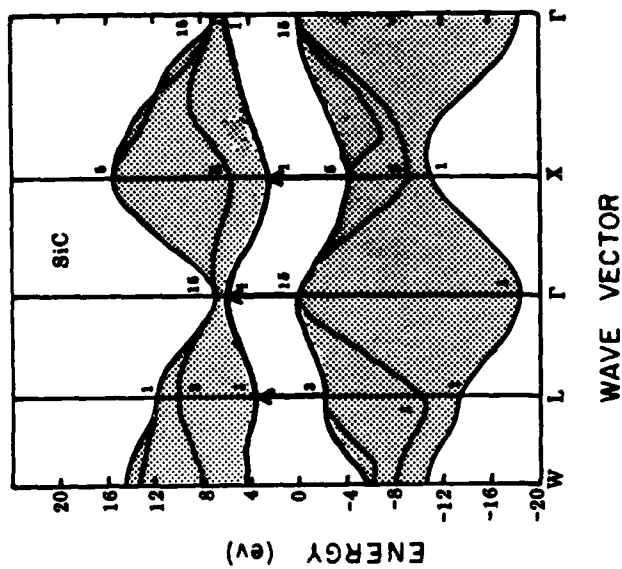
Other modeling approaches may seem more appropriate. For example, utilizing sophisticated surface science techniques, Brillson (8) has been able to extend the correlation between metal/semiconductor interfacial heats of reaction and Schottky barrier heights. This model, however, says little about which surface properties of the original surfaces are desirable. Theoretical models, such as Ferrante and Smith's (3) universal bonding model for metals, are conceptually simple but the calculations can be extensive and complex; in addition, the models are not easily verified with measurable electronic parameters. On the other extreme, semi-empirical and empirical models can be either too cumbersome (with a large number of adjustable parameters) or limited in scope.

The proposed model for this research will extend the basic concept from Phillips semiconductor model (4); i.e. the use of direct interband transition energies to predict bond formation energies (enthalpies of formation). The formation energy of any solid or interface, whether metallic, covalent, or ionic, is a function of the interband transition energies that occur at symmetry or "critical" points of the solid. To confirm this premise, the proposed interfacial bonding model will begin with Phillips semiconductor model. It will then be extended to transition metals, and conclude with simple polyvalent metals (i.e. aluminum).

3.1.2 Semiconductors

Phillips semi-empirical bonding model for Group IV tetrahedrally coordinated components was mentioned in the introduction, and will be presented briefly here for completeness. The model accurately predicts enthalpies of formation for the Group IV compounds; compounds which consist of nearly complete covalent bonding at the top of the column (e.g., C, Si) to

Crystal	$-\Delta H$ (Pauling)	$-\Delta H$ (spectro.)	$-\Delta H_{\text{expt}}$
BN*	13.6	63.6	60.8
BeO*	158.0	128.5	143.1
AlP*	24.8	22.2	39.8
CaAs	11.0	16.3	17
ZnSe	29.4	39.8	39
InSb	2.9	9.0	7.3
CdTe	4.4	25.1	22.1
ZnO*	140.1	72.5	83.2
AlAs*	17.3	17.3	27.8
GaP	17.3	24.8	24.4
ZnS	37.3	42.1	49.2
InP	11.0	20.3	21.2
CdS	29.4	35.8	36.7
AlSb	11.0	20.3	
GaSb	6.2	9.5	10.0
ZnTe	11.5	25.9	28.1
InAs	6.2	11.5	14.0
CdSe	22.5	30.9	32.6*
CuI*	8.3	14.9	16.2
CuBr*	16.6	22.7	25.0
CuCl*	27.8	34.9	32.8



(a)

(b)

Figure 6. (a) Electronic energy bands of β -SiC, arrows depict characteristic energy band transitions. (b) Values of ΔH (in Kcal/mole) according to the Pauling (molecular theory), Phillips (spectra) and actual calorimetric measurements (expt.).

increased metallic bonding at the bottom (e.g. Pb). Not only does the model incorporate covalent and metallic bonding, but ionic bonding as well.

With respect to the electronic properties such as conductivity, the semiconductor at low temperatures is insulating whereas at high temperatures, the semiconductor is conductive. The semiconductor forms a gap between occupied (valence) and unoccupied (conduction) electronic states, and it is these gaps at symmetry points that Phillips uses to predict bond energies. Energy band widths are also used to determine the degree of ionicity/covalency; decreasing the band width increases ionicity and increasing the band width increases covalency.

A theoretical energy band structure for SiC is shown in Figure 6a. At specific wave vectors, or symmetry points, characteristic energy transitions can occur between either lower or upper valence band levels to the conduction band. An absorption spectrum would have well delineated peaks corresponding to the energy transitions at symmetry points (refer to Figure 6b).

Phillips semi-empirical model for enthalpy of formation is as follows:

$$\Delta H_{AB} = \Delta H_0 \left[\frac{d_{Ge}}{d_{AB}} \right]^S f_i (AB) D$$

where: ΔH_0 = scaling constant

$\left[\frac{d_{Ge}}{d_{AB}} \right]$ = covalent energy not lost by dehybridization

f_i = ionic ordering energy

D = dehybridization factor

S = 4

Phillips' results for various semiconductor type materials are shown in Figure 6b and both Pauling and experimental thermodynamic data are included for comparison.

The enthalpy of formation for the as-received semiconductor or ceramic substrate will be evaluated with this technique. The details of the experimental technique will be discussed in the experimental section.

3.1.2 Metals

With increasing metallicity, such as the transition from carbon to lead in Group IV elements, the valence and conduction energy bands overlap and the clearly delineated gaps in semiconductors become less well-defined in metals. However, with the use of differential optical reflectance, Hummel (9) has been able to resolve structural features in the absorption spectra of noble metals where the spectra was otherwise featureless. Hummel has developed a technique to accentuate interband transitions in metals. The same type of interband transitions occur at symmetry points in semiconductors and are used successfully in the determination of enthalpies of formation.

The correlation between energy level position and/or energy level broadening, and the bonding energy in transition metals has been previously given by Friedel. Since there are a "large number" of energy levels close to the Fermi level in transition metal elements, the bonding energy gained by band broadening is the most important term in cohesion. According to Friedel (10), ΔH_{AB} in transition metals is accounted for by the broadening of the partially filled d-bands. Although Hummel has used modulated spectroscopy for determining transition energies in only noble metals, there is no reason why the technique can't be applied to the determination of transition energies in other metals, such as transition metals or simple polyvalent metals (e.g. aluminum).

3.2 Modulation Spectroscopy

3.2.1 General Concept

In modulation spectroscopy, the derivative of the unperturbed reflectivity (i.e. ϵ_2) is measured with respect to an external parameter. A variety of external parameters, such as electric field, pressure, temperature, and incident radiation wavelength can be used for the modulation of the band structure (11). With modulation, specific interband transitions, which occur at symmetry or critical points in the band structure, are enhanced above an otherwise featureless background. The background is caused by the allowed transitions at practically all points in the Brillion Zone.

The main advantages of the modulated spectra over conventional optical techniques are:

1. Enhancement or separation of energy interband transition at high symmetry points from the background.
2. Ability to eliminate undesirable influence of oxides and instrumental variations upon a spectra because of the differential nature of the technique.
3. No vacuum is needed (unless desired).

In contrast to conventional optical reflectance measurements of metals and alloys which lack sharp structure because of the energy band spreading that occurs in solids, modulated reflectometry can sharply define interband transition energies.

Hummel (9) has applied differential reflectometry to the study of surface properties and alloy formation; his modulating parameter is sample composition (i.e. addition of solute atoms to pure materials). Band structure changes are measured as a function of solute additions. This technique, along with thermorefectance, appears as the most likely candidate for characterizing the electronic structure/properties of solids and would compliment the work presented earlier by Phillips.

3.2.2 Simple Polyvalent Metals (i.e. Mg, Al, etc.)

According to Hummel, "critical" point interband transitions in metals can be resolved with modulation spectroscopy. According to Phillips and Friedel, these sample interband transitions can then be used to determine cohesive energies, enthalpies of formation in semiconductors and transition metals respectively.

The structural features in the optical spectrum for simple polyvalent metals are less clearly resolved than for transition metals or semiconductors. Structure in the optical absorption spectrum for polyvalent metals, however, is strongly influenced by electronic interband transitions between "parallel-bands". Just as Hummel used solute additions as the modulating parameter in noble metals, composition modulation in the polyvalent metal should enhance the "parallel-band" interband transitions above the background transitions.

Parallel-band gap energies have been theoretically determined as a function of close-packed direction, for a number of polyvalent metals (12). Plots of theoretical parallel-band gap versus heat of vaporization and surface tension are given in Figures 7 and 8. Since the correlation between interband transitions and enthalpies of formation for other types of metals was shown

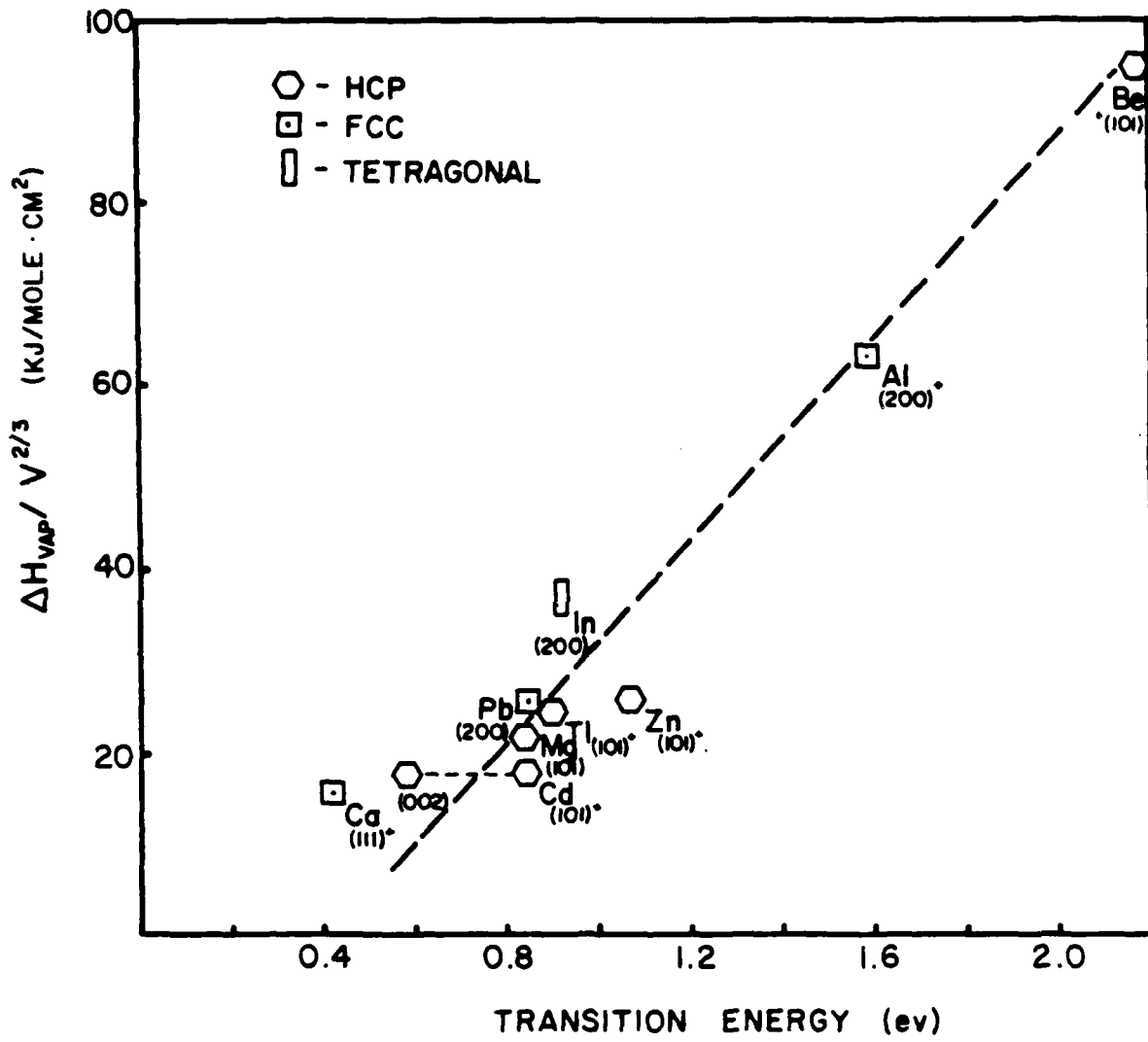


Figure 7. Theoretical "parallel-band" gap energies versus heat of vaporization.

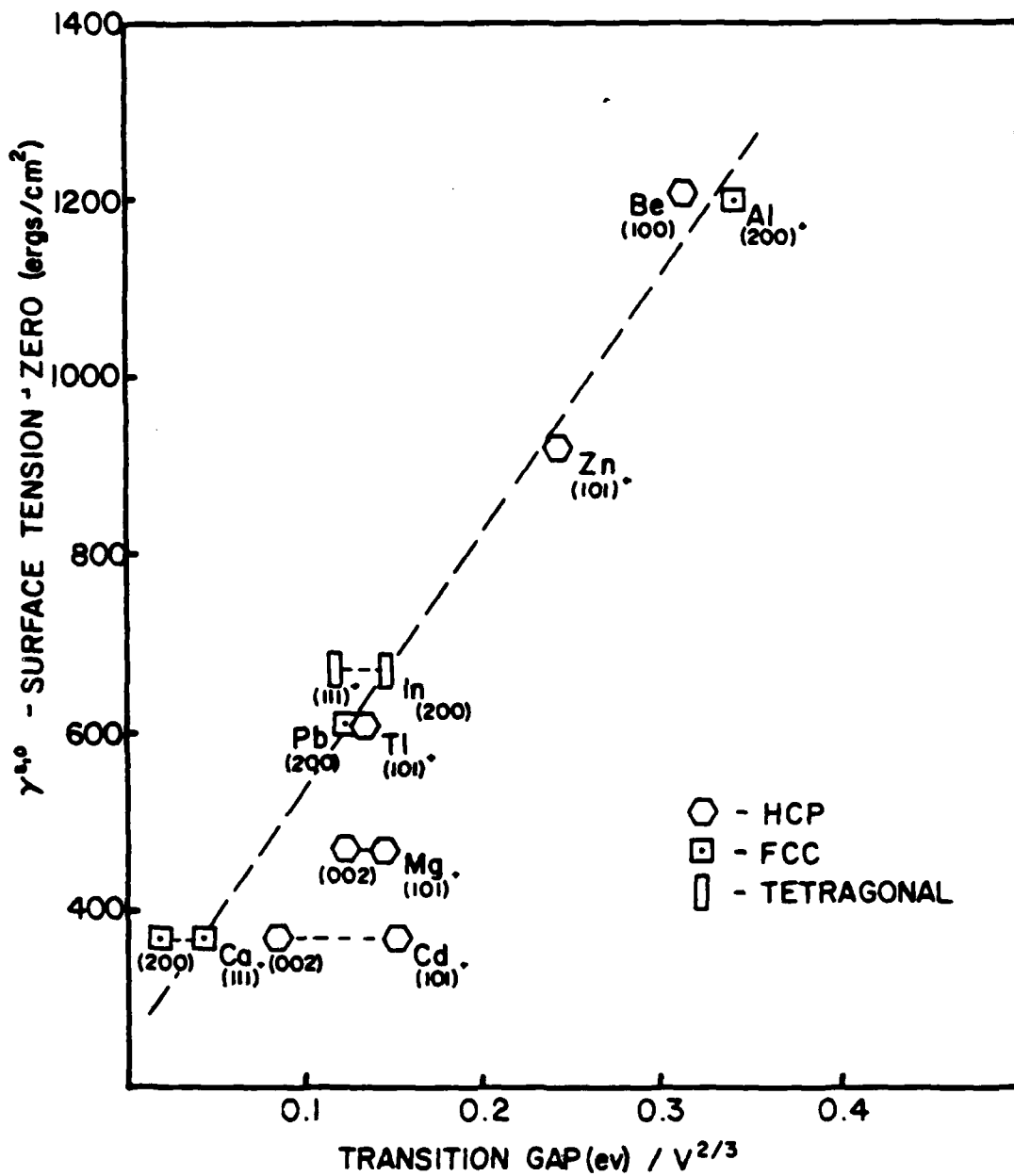


Figure 8. Theoretical "parallel-band" gap energies versus surface tension (0°K).

earlier, it is not surprising to see the same general trend for the simple polyvalent metals.

To theoretically predict interfacial bond strengths, the following method will be applied: 1) determine enthalpies of formation for both the semiconductor (ceramic) and the metal from the modulated reflectance measurement, 2) determine interfacial energies from the enthalpies of formation (from Miedema theory), and 3) use interfacial energies to calculate interfacial bond strengths and wettability parameters ($\gamma_{LV} \cos\theta$). These theoretical measurements will be compared to the experimental punch-die shear test measurements, as well as to enthalpies of formation of compounds that may form in the interphase region.

3.3 Optical Measurements of Interfaces

The experimental measurements described have been for the particular constituents involved and not for the actual interface. This is consistent with the objectives of the project, whereby interfacial properties of each constituent are determined from electronic measurements and used to predict the interfacial bond strength. However, owing to the unique properties of a semiconductor, such as silicon carbide, it may be possible to determine an enthalpy of formation of the actual interface.

Below approximately 7.75eV, the band gap, pure silicon carbide will be transparent to incoming radiation. As impurities are added to silicon carbide, the number of donor and acceptor levels increase and the minimum energy gap between the valence and conduction band will decrease. To insure optical transparency in the lower energy range (< 6.5eV), the silicon carbide must be pure.

Assuming the penetration depths for modulation reflectance are on the order of thousands of microns for a relatively pure silicon carbide and only 50-100A for metals, then the optical beams can be used to probe through a silicon carbide substrate and into the actual silicon carbide/aluminum interface. Under normal circumstances, the silicon carbide/aluminum interface is not a sharp but a diffuse region since reaction products and interdiffusion have extended the thickness of the interfacial region. To measure the optical properties of the interface with the modulation reflectance technique then, a series of interphase regions will be manufactured; each having a different degree of interfacial reactivity or sharpness.

Sharp interfaces created by solid state bonding can be heat treated to produce varying degrees of interfacial diffusion and reactivity so that the degree of chemical reactivity or diffusion can be used as the modulating parameter in these experiments. The reflectance spectra is expected to shift as the extent of interfacial reactivity increases, and it is these shifts which can be used to determined the interfacial energies.

3.2.3 Description of the Differential Spectrometer

The differential reflectometer measures the normalized difference between the reflectivities of two specimens which are mounted side by side with virtually no gap in between. The incident light from the double monochromator is unpolarized and is alternately deflected to one or the other sample by means of a vibrating mirror or the oscillation of the actual sample. Reflected light is directed toward the photomultiplier tube (PMT) and the output signal from the PMT consists of a direct current component, modulated by a 60 hz square wave.

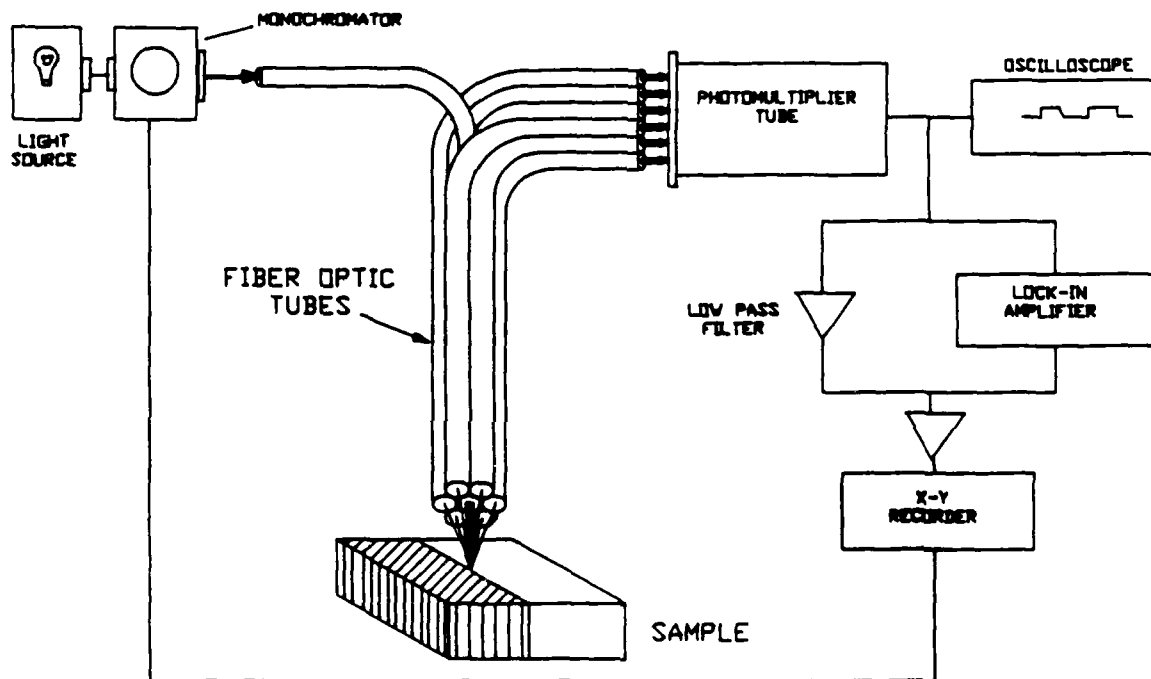


Figure 9. Schematic of the proposed spectrometer.

Depending on the electronics of the instrument, a plot of $\Delta R/R$ versus wavelength can be generated automatically, completing the entire scan in less than 5 minutes. Most spectrometers are complex, with a large number of mirror and prisms, and difficult to calibrate. One means for simplifying the optics and the same time improve the sensitivity and accuracy of the instrument is to use fiber optics. A schematic of the spectrometer for this study is shown in Figure 9. The only major limitation of this design is the optical response of the quartz fibers. Above about 8.5eV, the optical transitions in the quartz begin to interfere with the measured transition energies, resulting in excess background noise.

4.0 FUTURE WORK

There will be continued research to investigate the infiltration kinetics and bond strength of metal matrix composites in three different areas: 1) infiltration of porous compacts by liquid aluminum alloys, 2) infiltration of liquid aluminum into fine-bore capillaries of SiC, and 3) electronic characterization of solid substrates.

1. Porous Compacts

- a. Future tests are needed to quantify both temperature and pressure dependence for the initiation of infiltration. Investigations of the significance of incubation time and threshold pressure and their relation to interfacial reactions will continue.
- b. Additional tests will be conducted to study the effect of infiltrant composition on infiltration behavior. These compositional variations will assist in understanding the incubation time and threshold pressure.
- c. SiC particles coated with electroless copper (and other metals depending upon early results) will be infiltrated. These coated particles, which have been sintered to minimize redistribution during infiltration, will provide insight regarding infiltration rates, incubation times and threshold pressures.

2. Capillary/Tube Bundle

These experiments are separated into two different categories; static rise and dynamic infiltration measurements.

- a. Static rise experiments are used to measure a wettability parameter $\gamma_{LV} \cos \theta$, where γ_{LV} is the liquid/vapor surface tension and θ is the contact angle. Tests are continuing to measure $\gamma_{LV} \cos \theta$ as a function of temperature and alloy addition. Since there has been a question as to whether "true equilibrium" is maintained in these tests, $\gamma_{LV} \cos \theta$ versus time measurements are also being conducted.

- b. As presented in the report, the dynamic infiltration tests will not only verify the predicted infiltration rates but the samples from each test will be used to measure an interfacial shear strength. Measurements are currently being made for pure aluminum, but will be extended to include Al-Li, Al-Mg, and Al-Si alloys.

3. Electronic Characterization of Solid Substrates

- a. A key objective in this phase of the work will be the measuring of a reflectance spectrum with a spectrophotometer. Preparation of the experimental equipment is underway.

- b. Pure copper and copper-zinc standards have been prepared and the aluminum or aluminum alloy and SiC samples will be prepared.

- c. Preparation is also being made to solid state bond aluminum-coated SiC single crystals to pure aluminum and aluminum alloy substrates. These samples will also be subsequently tested with the modulated optical reflectance technique.

5.0 ACKNOWLEDGEMENTS

We wish to gratefully acknowledge the support of Steve Fishman and the Office of Naval Research. In addition, the contributions from Dr. Martins and the efforts of Bruce Lanning, Paul Campbell and John Seitz are appreciated.

6.0 REFERENCES

1. Maxwell, P.B., "The Infiltration Behavior of Aluminum into Silicon Carbide Compacts", CSM Thesis No. T-3396, Colorado School of Mines, Golden, CO, April, 1987.
2. Martins, G.P., Olson, D.L., and Edwards, G.R., "Modeling of Infiltration Kinetics for Liquid Metal Processing of Composites", Metallurgical Transactions, vol. 19B, (1988) pp. 95-111.
3. Smith, J.R., and Banerjee, A., "Origins of the Universal Binding-Energy Relation", Phys. Rev. B, vol. 37, no. 12 (1988), pp. 6632; Ferrante, J., and Smith, J.R., "Theory of the Bimetallic Interface", Phys. Rev. B, vol. 31, no. 6 (1985), pp. 3427.
4. Phillips, J.C. and Van Vechten, J.A., "Spectroscopic Analysis of Cohesive Energies and Heats of Formation of Tetrahedral Alloy Coordinated Semiconductors", Phys. Rev. B., vol. 2, no. 6 (1970), pp. 2147.
5. Phillips, J.C., "Ionicity of the Chemical Bond in Crystals", Rev. Mod. Phys., vol. 42, no. 3 (1970), pp. 317.
6. Miedema, A.R., "Surface Energies of Solid Metals", Z. Metallkde, vol. 69, (5), (1978), pp. 287.

7. Miedema, A.R., and den Broeder, J.A., "On the Interfacial Energy in Solid-Liquid and Solid-Solid Metal Combinations", vol. 70 (1), (1979), pp. 14.
8. Brillson, L.J., "Advances in Understanding Metal-Semiconductor Interfaces by Surface Science Techniques", J. Phys. Chem. Solids, vol. 44, no. 8 (1983), pp. 703.
9. Hummel, R.E., "Differential Reflectometry and Its Application to the Study of Alloys, Ordering Corrosion, and Surface Properties", Phys. Stat. Sol. (a), vol. 76, no. 11 (1983), pp. 11.
10. Friedel, J.D., "Electronic Structure of Primary Solid Solutions in Metals", Advances in Phys., vol. 3, (1954), pp. 446-507.
11. Seraphin, B.O., "Electroreflectance", Semiconductors and Semimetals, Ed. by Willardson, R.K., and Beer, A.C., vol. 9, Academic Press (1972), pp. 1.
12. Harrison, W.A., "Parallel-Band Effects in Interband Optical Absorption", Phys. Rev. vol. 147, no. 2 (1966), pp. 467.
13. Delannay, F., Froyen, L., Deruyttere, A., "Review: The Wetting of Solids by Molten Metals and its Relation to the Preparation of Metal-Matrix Composites", J. Mater. Sci., (1987), pp. 1.
14. Bailey, G.L., and Watkins, H.C., J. Inst. Met., vol. 80, (1951-52), pp. 57.

15. Miedema, A.R. and den Broeder, J.A., Z. Metallkde, vol. 70 (1979), pp. 14.
16. Humenik, Jr., M., and Kingery, W.D., J. Amer. Ceram. Soc., vol. 37 (1954), pp. 18.
17. Naidich, J.V., Prog. Surf. Membr. Sci., vol. 14 (1981), pp. 353.
18. Van Vlack, L.H., "The Metal-Ceramic Boundary", Metals Engineering Quarterly (ASM), (1965), pp. 7.
19. Kohler, W., "Untersuchungen zur Benetzung von Al_2O_3 and SiC - Kristallen durch Al und Al-Legierungen", Aluminum, vol. 51 (1975), pp. 443.
20. Warren, R., and Andersson, C.H., "Silicon Carbide Fibers and Their Potential for Use in Composite Materials Part II", Composites, vol. 15, no. 2 (1984), pp. 101.
21. Froyen, L., and Deruyttere, A., "Metallic Composite Materials and Microgravity", Proc. of the 4th Europ. Symp. on Materials Sci. under Microgravity (Spain), (1983), pp. 31.
22. Laurent, V., Chatain, D., and Eustathopoulos, N., "Wettability of SiC by Aluminum and Al-Si Alloys", J. Mater. Sci. (1986), pp. 244.
23. Bermudez, V.M., "Auger and Electron Energy-Loss Study of the Al/SiC Interface", App. Phys. Lett., vol. 42, no. 1 (1983), pp. 70.

24. Van Bommel, A.J., Crombeen, J.E., and Van Tooren, A., "Leed and Auger Electron Observations of the SiC (0001) Surface", Sur. Sci., vol. 48 (1975), pp. 463.
25. Eustathopoulos, N., "Energetics of Solid/Liquid Interfaces of Metals and Alloys", Int. Metals Rev., vol. 28, no. 4 (1983), pp. 189.
26. Choh, T., and Oki, T., "Wettability of SiC to Aluminum and Aluminum Alloys", Mater. Sci and Technol., vol. 3 (1987), pp. 378.
27. Yupko, V.L., Gusliencko, Y.A., Monastyreva, N.I., and Dvernikova, T.N., "Character of Wetting of Some Refractory Compounds by Melts of Eutectic Composition", Poroshkovaya Metallurgiya, no. 3 (243), (1983), pp. 52.
28. Naidich, Y.V., Chubashov, Y.N., Ishchuk, and Krasovskii, V.P., "Wetting of Some Nonmetallic Materials by Aluminum", Poroshkovaya Metallurgiya, no. 6 (246), (1983), pp. 67.

APPENDIX I

INFILTRATION AND WETTABILITY

It will be shown that the factors which control the strength and stability of the solid-solid interface will also influence the wetting or the formation of strong bonds at the solid-liquid interface. Enhanced wetting usually induces enhanced strength of the metal/ceramic interface.

To understand wetting and infiltration, a brief outline of the relevant thermodynamics of interfaces will be given, followed by a discussion of the energetics at solid-liquid interfaces. Finally, a consideration will be given to those factors which will enhance wetting and infiltration in metal/matrix composites.

Interfacial Thermodynamics

In the literature, the concepts of surface tension and surface free energy are not clearly distinguished and to a certain extent, these terms have been used interchangeably. A surface tension between a pure liquid and a gas may be explained as follows.

Atoms at the liquid surface are attracted either inward or parallel to the surface by adjacent atoms. This force is not counterbalanced by an opposing outward force because of the lower density of atoms in the vapor phase. Hence, work has to be done to bring atoms from the bulk to the surface, and this additional energy of atoms at the surface is expressed as an amount of energy per unit surface area. To maintain equilibrium, the surface is envisioned as a membrane stretched under tension (i.e. a "surface tension").

The surface tension is defined thermodynamically as:

$$\gamma = \left(\frac{\partial F}{\partial A} \right)_{T, V, n_i} \quad (1)$$

Using the Gibbs model, the surface tension can also be expressed as:

$$\gamma = \frac{F^s}{A} - \sum \Gamma_i \mu_i^s \quad (2)$$

where Γ = surface adsorption coefficient of species i .

When the position of the dividing interface is chosen such that $\sum \Gamma_i \mu_i^s = 0$, γ becomes equal to the surface free energy, F^s , per unit surface area.

Whereas the surface free energy is an abstract quantity, the surface tension of a liquid is measurable.

The surface tension of a solid does not fit the stretching membrane analogy because of the limited mobility of the atoms (i.e. different surface energies on different crystallographic faces). For solids, the concept of surface tension will be referenced to the surface free energies, since surface tensions can't easily be measured (the dividing surface or interface must be chosen such that $\sum \Gamma_i \mu_i^s = 0$).

For the solid/liquid interface, it is helpful to think in terms of the work of adhesion, W_a , where:

$$W_a = \gamma_{SV} + \gamma_{LV} - \gamma_{SL} \quad (3)$$

The work of adhesion is equal to the work that must be performed in order to separate one unit surface area of the two phases in vacuum. This is a good qualitative measure of the binding strength between the liquid metal and ceramic phases.

Interfacial tension can also be understood in terms of surface excess quantities, Γ_i , or adsorption/segregation at the liquid surface. If the variation of γ with the change in the bulk activity of a component A is known, then the surface adsorption of component A can be calculated by the following Gibbs absorption equation:

$$\Gamma_{i,1} = -\frac{1}{RT} \frac{d\gamma}{a(\ln a_2)} \quad (4)$$

In other words, if the addition of component A decreases the surface tension of the bulk solution, then component A will selectively segregate to the surface. Hence, surface active agents which selectively segregate to the surface can be used to enhance wettability according to the above relation.

The wettability of a solid by a liquid is characterized by the Young equation:

$$\gamma_{LV} \cos\theta = \gamma_{SV} - \gamma_{SL} \quad (5)$$

where: θ is the angle of contact between the solid and liquid.

In a vacuum, where there is no adsorption of the liquid components onto the solid, the following equation for the work of adhesion, W_a , is used.

$$W_a = \gamma_{LV} (1 + \cos\theta) \quad (6)$$

γ_{LV} appears in the above equation because of its relation to γ_{SL} .

Lowering the surface tension of the liquid, i.e. γ_{LV} , will not necessarily decrease the work of adhesion or increase the rate of infiltration.

In practice, when a liquid is brought in contact with a solid, irreversible phenomena, such as reactions or diffusion, will occur until

equilibrium is finally reached. A thin layer of oxides, or impurities can form between the two bulk phases which will affect the local equilibrium at the interface. The kinetics of this type of system are temperature dependent, relating to the dissolution of oxides (impurities) on the surface. The use of the wettability relations in this section assumes equilibrium between the solid, liquid, and gas phases, and when considering liquid metal/ceramic systems, the true equilibrium phenomena can be very sluggish and complex.

The dynamics of liquid metal infiltration into a ceramic capillary network will be discussed in the proposed model selection. The concepts of wettability, even for a non-wetting system such as Al/SiC, will be used in the discussion of the infiltration model.

Energetics of the Solid/Liquid Interface (SiC/Al)

According to the equation for the work of adhesion, W_a , above, the condition for spontaneous spreading occurs when $W_a \geq 2\gamma_{LV}$. A liquid wets a solid surface only if the energy of the bonds that are created across the interface exceeds the surface tension of the liquid (13). In metal-metal systems, mutual solubility or the formation of intermetallic compounds is considered a necessary condition for wetting (14). This concept of mutual solubility (and/or the formation of intermetallic compounds) has been related to the classical exchange energy, Ω , in regular solution theory by Miedema and den Broeder (15); the higher the affinity of two metals for each other, the lower the exchange energy and the lower γ_{SL} (higher W_a).

The solid/liquid interaction energies of the metal/ceramic systems are dominated by chemical interactions as opposed to other interactions such as dispersion forces, which are physical interactions.

The wettability of molten metals on ceramic substrates is controlled by the formation (or absence) of oxides at the respective surfaces. For instance, SiC forms a stable oxide and in most cases, it is this oxide that controls the wetting behavior of the solid. Therefore, if the surface of SiC is considered as an oxide, the work of adhesion, W_a , for a liquid metal on this oxide surface is expected to increase if the metal has an increasing affinity for oxygen; i.e., a large negative standard free energy of oxide formation (16).

Another result concerns the drastic increase of W_a with increasing concentration of oxygen in the melt. According to Naidich (17), the oxygen in the melt creates $Me^{2+}O^{2-}$ complexes which selectively absorb at the metal/ceramic interface; the higher the affinity of the metal for oxygen, the lower the solubility of the $Me^{2+}O^{2-}$ complexes and the higher the interfacial activity. The Me^{2+} reacts with the oxygen anions of the solid surface to form a strong interfacial bond.

In another finding (18), the work of adhesion between a metal/ceramic interface is shown to increase when the ceramic is saturated with the oxide of the molten metal. The saturation of the ceramic phase with the metal oxide insures that there are primary ionic bonds across the interface; this is similar to the case described above as discussed by Naidich. Regardless of the nature or mechanics of interfacial bond formation (i.e. oxide, carbide, etc.), whichever combination of factors leads to a gradual transition (structural composition) across the interface, a low interfacial energy, or an increase in the degree of coherency, then the externally supplied energy to separate the interface will be high.

The problem of oxide formation is not just with the ceramic. The molten metal can also form a surface oxide which will affect the kinetics of

wetting. Since aluminum can form a stable oxide, the molten metal is usually covered with an oxide layer, a layer which will retard wetting by preventing metal-solid contact. Even during infiltration, when the oxide layer appears to break and "slide" from the liquid/gas to the liquid/solid interface, a new monolayer of aluminum oxide will form to keep pace with the infiltration front. The threshold temperature at 950-1000C, where aluminum wets the SiC surface (i.e. $\theta < 90^\circ$), may in fact be due to the penetration of liquid aluminum through the oxide barrier. In general then, when investigating the wettability or infiltration behavior of molten metals on ceramic substrates, the question of oxides or impurities will have a significant effect on the observed results.

The threshold or transition temperature of 950-1000°C, alluded to above, has been reported by a number of investigators (19,20,21). From the melting point of pure aluminum up to approximately 950°C, pure aluminum does not "wet" pure SiC, i.e. $\theta > 90^\circ$. Above approximately 1000°C, pure aluminum will then "wet" SiC, i.e. $\theta < 90^\circ$. Although this observation is well founded in the literature, there is still some doubt as to the conditions at the solid, liquid, and gas interfaces when the contact angle measurements were made and whether oxides or impurities were present.

Froyen (21), Kohler (19), and other researchers (20) support the concept of a transition temperature. Froyen, for instance measured the change in contact angle as a function of time and temperature. At temperatures below approximately 950°C, the angle stabilized in less than 20-25 minutes (these tests were continued for more than an hour). Froyen used "pure" α -SiC single crystals and "pure" aluminum in high vacuum and microgravity conditions (there is nothing to indicate that oxides may not have been present).

Work by Eustathopoulos (22), however, contradicts the previous observation that aluminum does not wet SiC below 950°C. In 2-hour tests, Eustathopoulos measured the change in contact angle with time. He found that more than 100 minutes were required to obtain a constant angle and that for pure aluminum, the contact angle dropped below 90° in less than 40 minutes. Eustathopoulos used high purity aluminum and cleaved, polished, α -SiC single crystals in an ultra-high vacuum. When plotted as a function of temperature, the contact angles, measured after the first 15 minute holding times, exhibited a transition from non-wetting to wetting behavior.

It is not clear what role oxides have in controlling wetting, or the incubation times and rates in the infiltration process. With respect to the actual infiltration process, liquid metal is usually in contact with the solid ceramic for less than 15 minutes. To improve or enhance the kinetics of infiltration at temperatures below 950°C, then any surface pre-conditioning of the SiC or aluminum must instantaneously change the local equilibrium conditions at the interface in order to have an effect.

Before considering techniques to enhance the infiltration or wettability of the SiC/Al system, a note should be made on the nature of the SiC surface. In the event an uncontaminated pure SiC surface could be generated, what type of surface interaction with pure aluminum would be expected? Bermudez (23) reported such an investigation for the Al/SiC interface in an ultrahigh vacuum chamber using Auger and energy loss spectroscopy. When heat treated at temperatures as low as 800°C, pure silicon carbide will develop a graphitic layer at the surface which is somewhat coherent with the underlying matrix (24). This carbon enriched layer can then interact with the aluminum. Bermudez vapor-deposited aluminum onto pure silicon carbide substrates, annealed the samples at different temperatures, and observed the interfacial

reactions. Below the melting point of aluminum (i.e. approximately 650°C), the Al-Al interaction was high and islands of aluminum or nucleation sites for further aluminum growth were observed to form. Above the melting point of aluminum, aluminum reacted with the excess surface carbon to form the stable Al_4C_3 .

The molten aluminum/silicon carbide interface is complex. As shown above, if pure aluminum came in contact with pure SiC, a stable carbide, Al_4C_3 would form, and any measurement of interfacial energies would involve pure aluminum in contact with an aluminum carbide. The practical interpretation of Al/SiC wettability will incorporate the inherent contamination problems and the evaluation of wetting enhancement techniques, presented in the next section, will assume varying degrees of contamination at the Al/SiC interface.

Techniques to Enhance Infiltration/Wettability of SiC/Aluminum Composite

In general, the wettability of covalent carbides, such as SiC and B_4C by metals follows the same dependence as the wettability of carbon by metals (14). On carbon, metal wetting is enhanced either by lowering γ_{LV} or forming a carbide. Alkali metals, such as lithium and sodium, can induce wetting on carbon because of the low value of surface tension, γ_{LV} . Boron, aluminum, and silicon can form carbides with covalent metal-carbon bonds. Likewise, transition metals react strongly with carbon to form transition metal carbides. This involves the transfer of electrons of carbon to the d-shell of the metal.

Although lithium or titanium can be added to the aluminum melt, the wettability of SiC can still be hindered by the presence of oxides. However, on carbon, lithium has been shown (25) to weaken the diffusion barrier created

by the Al_2O_3 film on liquid aluminum. This is consistent with the Gibbs equation, where surface active agents can selectively segregate to the surface and reduce γ_{LV} (increase wetting). It might be argued that in infiltration, the interface moves faster than the components can diffuse to the surface; but, for many of the "surface active" agents, this is not a factor.

Wettability of SiC by aluminum can be improved by the addition of transition metals to the melt. Choh and Oki (26) showed that, in the presence of transition metals, the wetting rate increased and the incubation time decreased (10-40% depending on element) for aluminum on SiC (The incubation time for pure aluminum was about 205 sec.). They further proposed that the wetting rate was determined by the disassociation of SiC since the same value of activation energy for the wetting process was found for pure aluminum, Al-Ti, Al-V, and Al-Zr (i.e. approximately 327 KJ/mole).

It has been shown (27,28) that a decrease in the thermodynamic stability of the base material leads to an increase in the wetting of carbides by liquid metals. Also, when considering a transition metal carbide and covalent carbide of equal stability, the transition metal carbide will be more easily wetted by liquid metals because of the higher proportion of metallic bonding (27). Hence, since SiC (52.1 KJ/mole) has a lower heat of formation than B_4C , aluminum will wet SiC more easily than B_4C . This concept is not surprising since wetting is related to the formation of chemical bonds at the interface; the greater the affinity of liquid metal atoms for the atoms in the solid, then the greater the wettability.

A common technique to enhance the metal wetting of the ceramic substrate is to use coatings on the ceramic. Nickel, copper, silver, and chromium are a few metal coatings that have been used in the SiC/Al system. Nickel forms

stable intermetallic compounds whereas silver can enhance wettability by changing γ_{LV} . Fluoride compounds, such as NaF or K_2ZrF_6 , are used to enhance the wettability of aluminum by breaking down the Al_2O_3 skin that forms on the aluminum melt. Coatings are used not only to enhance wetting, but in most cases, they are used to provide a diffusion barrier. In this sense, the coatings will prevent the formation of brittle intermetallics and improve the properties of the interface.

APPENDIX II

BONDING AT THE METAL/CERAMIC INTERFACE

The internal energy, or enthalpy of formation, is a measure of the binding energy or bonding strength of a solid. Chemical bonding models presented thus far are explained in terms of enthalpies of formation, regardless of whether the solid is comprised of similar or dissimilar atoms. To understand the properties and bonding behavior at the solid-solid and solid-liquid interface, the enthalpies of formation will have to be presented in terms of interfacial energies. Miedema (7) developed a method for determining the interfacial energy in solid-liquid and solid-solid metal combinations in terms of the internal heats of formation of a compound or element. This approach will be used to link together enthalpies of formation and interfacial energies.

Interfacial Bond Strength

In the bonding of two dissimilar metals, Miedema defines an adhesion energy, $\Delta\gamma_{AB}$, the energy decrease per unit contact area, when two clean surfaces of metals A and B are replaced by an A-B contact:

$$-\Delta\gamma_{AB} = \gamma_A^{S,0} + \gamma_B^{S,0} - \gamma_{AB}^{SS} \quad (1)$$

where γ_{AB}^{SS} is defined as:

$$\gamma_{AB}^{SS} = 0.15 (\gamma_A^{S,0} + \gamma_B^{S,0}) + \gamma_{CHEM}^{SS} \quad (2)$$

and γ_{CHEM}^{SS} includes all interaction effects between A and B atoms (i.e. chemical interaction term).

According to Miedema, this term is determined by the following expression:

$$\gamma_{\text{CHEM}}^{\text{SS}} = 2.5 \times 10^{-9} \frac{\Delta H_{\text{SOL}}^i}{V_i} \quad (3)$$

Substituting (2) and (3) into equation (1), the interfacial bond strength, $-\Delta\gamma_{\text{AB}}$, is given by:

$$-\Delta\gamma_{\text{AB}} = 0.85 (\gamma_{\text{A}}^{\text{S},0} + \gamma_{\text{B}}^{\text{S},0}) - 2.5 \times 10^{-9} \frac{\Delta H_{\text{SOL}}^i}{V_i} \quad (4)$$

In the above expression, the surface energies for the solid metals, $\gamma_{\text{A}}^{\text{S},0}$ and $\gamma_{\text{B}}^{\text{S},0}$ are the most important terms whereas the second term is either a small positive or negative contribution. At zero temperature, the surface energy of the solid can be related to the heat of vaporization by the following expression:

$$\gamma_i^{\text{S},0} \propto \frac{Q_i \Delta H_{\text{VAP}}^{\text{S},0}}{V_m^{2/3}} \quad (5)$$

Therefore, once $\Delta H_{\text{VAP}}^{\text{S},0}$ and ΔH_{SOL}^i have been determined, a measure of the interfacial bond strength can be calculated from equation (4). This development from Miedema provides the link between interfacial bond strength and enthalpies of formation

WETTABILITY

The relationship between enthalpies of formation and interfacial energies can be extended to include the interaction between a solid and liquid; i.e., the solid/liquid interfacial energy. The wettability of a liquid metal in contact with a solid ceramic substrate could be understood in terms of the enthalpies of formation of the particular components. According to Yupko et

al. (27), the wetting of the metal-like compounds improved with decreasing heat of formation. It was shown that a decrease in the thermodynamic stability of the base material leads to an increase in the "nonequilibrium" part of the work of adhesion and hence to an improvement in the wetting in a system. Aside from this specific example, it is apparent that heats of formation should correlate with wetting tendencies.

The correlation between enthalpies of formation and solid/liquid interfacial energy begins with the Young and Dupre equation where for a liquid in contact with a solid:

$$\gamma_{LV} \cos\theta = \gamma_{SV} - \gamma_{SL} \quad (6)$$

where γ_{LV} = liquid/vapor surface tension

γ_{SV} = solid/vapor surface tension

γ_{SL} = solid/liquid surface tension

θ = contact angle between solid and liquid

Miedema then divides the interfacial energy between a solid A and liquid metal B into a physical and chemical contribution:

$$\gamma_{AB}^{SL} = (\gamma_{SL}^{\prime})_A + (\gamma_{SL}^{\prime\prime})_B + \gamma_{CHEM}^{SL} \quad (7)$$

where: $(\gamma_{SL}^{\prime})_A = 2.5 \times 10^{-9} \frac{\Delta H_f}{V_m^{2/3}}$

$$(\gamma_{SL}^{\prime\prime})_B = \frac{S^* T_f}{V_m^{2/3}} \approx 0.52 \times 10^{-7} \frac{T}{V_m^{2/3}}$$

(S^* - configurational entropy of atoms in liquid near surface of solid)

and γ_{CHEM}^{SL} is the same as γ_{CHEM}^{SS} given previously for the interfacial bond strength.

Collecting terms and substituting, $\gamma_{LV} \cos\theta$ could then be described by the following equation:

$$\gamma_{LV} \cos\theta = \frac{1}{V_m^{2/3}} (A \Delta H_{VAP}^{S,0} - B(\Delta H_f)_A - CT) - D \frac{\Delta H_{SOL}^{AB}}{V_{AB}} \quad (8)$$

$\gamma_{LV} \cos\theta$ is a measure of the wettability of a system and can be determined in terms of the enthalpies of formation of a system.

From the analysis of Miedema, an approximate method is given which relates enthalpies of formation to both the interfacial bond strength and the wettability of a solid/liquid system. The accuracy of the method is then dependent upon the determination of the various enthalpies of formation given in the above expression. Since the evaluation of the interfacial bond strength and the wettability parameter, $\gamma_{LV} \cos\theta$, from the enthalpies of formation is reasonably straightforward, the major emphasis in this project will be the determination of the enthalpy of formation in terms of a measurable electronic parameter.